CT ventilation imaging derived from breath hold CT exhibits good regional accuracy with Galligas PET

Enid M. Eslick [a], John Kipritidis [a,b], Denis Gradinscak [c], Mark J. Stevens [b,d], Dale L. Bailey [c,e], Benjamin Harris [d,f], Jeremy T. Booth [b,d], Paul J. Keall [a]

[a] Radiation Physics Laboratory, Sydney Medical School, University of Sydney, Camperdown; [b] Northern Sydney Cancer Centre, Royal North Shore Hospital; [c] Department of Nuclear Medicine, Royal North Shore Hospital; [d] Sydney Medical School – Northern, University of Sydney; [e] Faculty of Health Sciences, University of Sydney, Lidcombe; and [f] Department of Respiratory Medicine, Royal North Shore Hospital, Australia

Keywords: CT ventilation imaging, Galligas PET, Deformable image registration, Lung cancer

Corresponding Author :: Radiation Physics Laboratory, Sydney Medical School, The University of Sydney, Room 474, Blackburn Building D06, NSW, 2006, Australia.
E-mail address: paul.keall@sydney.edu.au (P.J. Keall).
URL: http://sydney.edu.au/medicine/radiation-physics (P.J. Keall).

Sources of funding

This work was supported by an NHMRC Australia Fellowship and a Cancer Institute NSW Early Career Fellowship

Acknowledgements

The authors thank the staff from the Royal North Shore Hospital's Nuclear Medicine, Radiation Oncology and Respiratory Medi- cine Departments. Finally, our thanks and gratitude go to the patients who volunteered their time to participate in this study.

Conflict of interest

Paul Keall is an inventor of a US patent on CT ventilation (#7668357). This patent is owned by Stanford University and is unlicensed.

Abstract

Background and purpose: CT ventilation imaging (CTVI) derived from four dimensional CT (4DCT) has shown only moderate spatial accuracy in humans due to 4DCT image artefacts. Here we assess the accuracy of an improved CTVI using high quality exhale/inhale breath-hold CT (BHCT).

Materials and methods: Eighteen lung cancer patients underwent exhale/inhale BHCT, 4DCT and Galligas PET ventilation scans in a single imaging session. For each BHCT and 4DCT scan, we performed deformable image registration (DIR) between the inhale and exhale phase images to quantify ventilation using three published metrics: (i) breathing induced lung density change, $CTVI_{DIR-HU}$ (ii) breathing induced volume change $CTVI_{DIR-Jac}$ and (iii) the regional air-tissue product, $CTVI_{HU}$ Spatial accuracy was reported as the voxel-wise Spearman correlation r between CTVI and Galligas PET.

Results: For BHCT-based CTVIs ($N = 16$), the $CTVI_{DIR-HU}$, $CTVI_{DIR-Jac}$ and $CTVI_{HU}$ methods yielded mean (range) r values of 0.67 (0.52–0.87), 0.57 (0.18–0.77) and 0.49 (0.14–0.75) respectively. By comparison the 4DCT-based CTVIs ($n = 14$) had values of 0.32 (−0.04 to 0.51), 0.16 (−0.31 to 44) and 0.49 (0.20–0.77) respectively.

Conclusions: High quality CT imaging is a key requirement for accurate CT ventilation imaging. The use of exhale/inhale BHCT can improve the accuracy of CTVI for human subjects.

Introduction

Ventilation imaging is extremely important in the planning of ablative pulmonary interventions in order to minimise treatment-induced parenchymal injury [1]. The last decade has seen several clinical investigations using computed tomography ventilation imaging (CTVI), which visualises air volume changes by analysing lung motion in respiratory-correlated four- dimensional CT (4DCT) [2–12]. Compared to the gold standard nuclear medicine ventilation imaging, CTVI offers the benefits of high resolution and high accessibility (especially in radiation oncology departments). Additionally CTVI is non-invasive and does not require the preparation of a radioaerosol or contrast agent.

Most CTVI implementations use deformable image registration (DIR) to calculate breathing induced air-volume changes in terms of regional lung density changes [2] or volume changes [3]. A major research focus for CTVI has been cross-modality validation in humans, that is, voxel-to-voxel comparisons of CTVI against a ground truth ventilation imaging modality such as ^{99m}Tc-based (DTPA and ‘‘Technegas”) single photon emission computed tomography (SPECT) [4,5,7,10,12] or ^{68}Ga-based (‘‘Galligas”) positron emission tomography (PET) [8,11,13]. In particular for radiother- apy treatment planning it is desirable to demonstrate strong voxel-level accuracy using the Spearman correlation *r*. Early validation studies using DTPA-SPECT showed relatively poor correlations ($r < 0.2$) and this has been attributed mainly to radioaerosol clumping in the central airways [4]. Kida et al. [10] reported much improved correlations between CTVI and DTPA-SPECT ($r \approx 0.4$) for 8 patients with non-severe clumping. The use of Galligas 4DPET/ CT, which uses a smaller radioaerosol less prone to clumping and provides better co-registration between the 4DCT and nuclear medicine scans, has also lead to improved voxel-level correlations ($r \approx 0{:}45$) [8,11].

Despite the improved results in recent CTVI validation studies, Hegi-Johnson et al. [12] found that the correlation between CTVI and ventilation SPECT was less than the agreement between ventilation SPECT and perfusion SPECT ($r \approx 0.6$ for 11 patients) and suggested that poor image quality of clinical 4DCT remains the major limitation on CTVI accuracy. It is known that 90% of clinical 4DCT scans suffer image artefacts >4 mm due to irregular breathing which manifest as anatomic blurring, duplication and truncation [14]. As a result of these imaging errors, CTVIs can vary depending on the 4DCT slice sorting method [15]. For surgical applications and assessment of global lung function, it is acceptable to mitigate this by assessing ventilation over larger regions of interest, for example lung thirds ($r \approx 0.45$) [6] or lung lobes ($r \approx 0.96$) [13,16]. For lung cancer radiotherapy however, a strong level of voxel-level accuracy still needs to be demonstrated.

The purpose of this study is to investigate an improved CTVI derived from pairs of exhale/inhale breath-hold CT (BHCT) scans free of motion artefacts. We perform the first head-to-head comparisons of BHCT-based CTVIs and 4DCT-based CTVIs using best-practice validation methodology. In particular the BHCT, 4DCT and Galligas PET scan components are all acquired in a single session on a combined 4DPET/CT scanner to minimise time delays and/or patient setup differences between the scans. The voxel level accuracy of CTVI is reported in terms of the Spearman *r* and compared against other CTVI validation studies. A schematic of the study design is shown in Fig. 1.

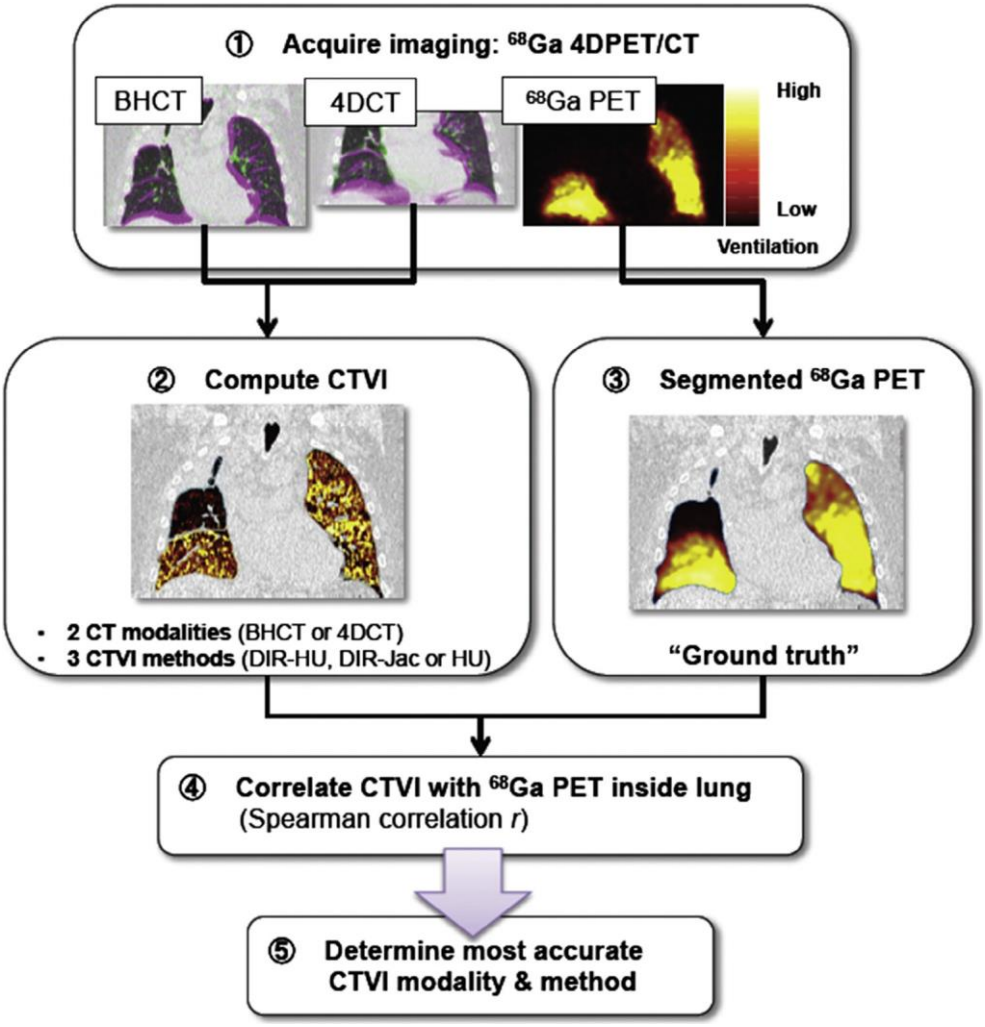

Fig. 1. Schematic of study design.

Methods

Patients

This study was a prospective single institution clinical trial approved by the health district ethics committee, (HREC/12/169) and registered with the Australian New Zealand Clinical Trials Registry (ACTRN12612000775819). The patient characteristics are described in (Table 1). A subset of this cohort was investigated in a previous CTVI study [13].

Table 1 Patient demographics in this study.

Parameter	**Value**
No. of patients	16
No. of men	8
No. of women	8
Age in years (range)	65 (54–73)
Lung function	
Mild COPD and D_{LCO} impairment	5
Moderate COPD and D_{LCO} impairment	6
Severe COPD and D_{LCO} impairment	5
FEV1%pred (mean ± SD)	81 ± 19
D_{LCO}%Pred (mean ± SD)	58 ± 15
Lung tumour staging (IASLC 2009)	
II	1
III	10
IV	3
Other	2
Tumour location	
Right Upper Lobe (RUL)	7
Right Middle Lobe (RML)	4
Right Lower Lobe (RLL)	4
Left Upper Lobe (LUL)	3
Left Lower Lobe (LLL)	0

Note: Except where indicated, data are means ± standard deviations. COPD = chronic obstructive pulmonary disease, FEV1%pred = percentage predicted forced expiratory volume in 1 second, D_{LCO}%Pred = percentage of predicted diffusing capacity of lung for carbon monoxide. IASLC = International Association for the Study of Lung Cancer.

Image acquisitions

All image acquisitions were performed on a Siemens Biograph mCT.S/64 PET/CT scanner (Siemens, Knoxville, USA) at the Royal North Shore Hospital between 2013 and 2015. A total of 14 4DCT scans, 16 inhale/exhale BHCT scans and 18 Galligas PET scans were successfully acquired for the 18 patients.

4DCT and Galligas PET acquisitions

The 4DCT and Galligas PET scans were acquired with the use of a respiratory motion sensor, the Anzai AZ-733V system (Anzai Medical Co., Tokyo, Japan) for retrospective sorting of the CT slices into 10 respiratory phase bins. As per departmental protocols, no immobilisation devices were used for the 4DCT or Galligas PET scans. Audio-visual biofeedback (Varian Medical Systems, Palo Alto, CA) was used to minimise irregular breathing during 4D imaging acquisitions.

4DCT scans were performed using a helical acquisition with settings 120 kVp, 80 mA to 200 mA; 0.5 s gantry rotation, ~0.09 pitch. The reconstructed 4DCT phase images had dimensions 512 x 512 with voxel spacing 0.96 x 0.96 x 1.7 mm^3 and were calibrated to Hounsfield Units (HU). Four patients had failed 4DCT reconstructions owing to irregular respiratory signal.
Details of the on-site Galligas production have been described previously [13,17]. The estimated inhaled activity was approximately 20 MBq. The Galligas PET scans (and corresponding attenuation correction CT) were acquired under free-breathing using a standard non-gated protocol. Galligas PET scans were acquired at 2 bed positions of 5 min each, with attenuation correction using a low dose CT (120 kVp; 0.8 pitch, 50 mAs). Galligas PET scans were reconstructed into a 400 x 400 matrix with 2.04 x 2.04 x 2.2 mm^3 voxel spacing using an iterative ordered-subset expectation maximisation (OSEM) algorithm. Reconstructed voxels had units of kBq/mL.

Breath hold CT acquisitions

For the exhale/inhale BHCT scans, patients were instructed to hold their breath at approximately 80% of maximum inhalation and exhalation. As with the 4DCT scans, no immobilisation was used during the BHCT acquisition. However Audiovisual Biofeedback was used to help guidance the breath hold procedure. Settings for the image acquisition were as follows: 120 kVp, 120 mAs, 0.8 pitch with a breath-hold time of 10 s. The field of view for the CT images was approximately 50 cm from the pharynx to the stomach. The reconstructed BHCT images had a voxel spacing 0.96 x 0.96 x 1.8 mm^3 with around 170 slices for each inhale or exhale image. Two patients had failed BHCT scans due to inability to comply with breath-hold instructions.

CTVI computation

For each patient and CT imaging modality (BHCT or 4DCT), we created 3 types of CTVI. The first two were based on B-spline DIR between the inhale and exhale CT phase images [2,3], whilst the third used a streamlined approach which did not require DIR [11]. All CT ventilation images were produced using VESPIR (‘‘VEntilation via Scripted Pulmonary Image Registration”), an open-source CTVI toolkit [18]. We applied a six stage DIR between the inhale (moving) image and the exhale (fixed) image using an intensity mean square error (MSE) image similarity metric and with motion field regularization $k = 1$. The DIR cost function was limited to lung voxels based on a coarse, threshold-based lung segmentation available in VESPIR. The segmentation method detects any aerated tissue inside the body contour using a fixed intensity cut-off of 250 HU.

Ventilation metrics

DIR based HU metric ($CTVI_{DIR-HU}$). The DIR-based HU metric, $CTVI_{DIR-HU}$, is based on Guerrero et al. [2]. This metric computes breathing induced air-volume changes as,

$$VI_{DIR-HU}(x) = \frac{HU_{exhale}(x) - HU_{*inhale}(x)}{HU_{*inhale}(x) + 1000}\rho_{scaling}(x)$$

Where $HU_{exhale}(x)$ and $HU_{*inhale}(x)$ give the CT number at voxel x in the exhale and (deformably registered) inhale phase images, respectively.

Our implementation of the $CTVI_{DIR-HU}$ method is slightly different to the original equation used by Guerrero et al. [2]. First, we have multiplied the right hand side by a factor HU_{exhale}=1000 in order to convert the original calculation of fractional air-volume changes to a calculation of absolute air volume changes at each voxel. We have also applied a tissue density scaling factor $\rho_{scaling}(x) = (HU_{exhale}(x) + 1000)/1000$ which takes a value in the range [0,1] and has been shown to improve the correlation of CTVI with Galligas PET [8]. This form of the equation is consistent with previous CTVI studies using Galligas and can be considered as a minor variant on the original equation.

DIR based Jacobian metric ($CTVI_{DIR-Jac}$)

The DIR-based Jacobian metric was developed by Reinhardt et al. [3] and is given by

$$CTVI_{DIR-Jac}(x) = \big((Jac(x) - 1)\big)$$

where $Jac(x)$ is the Jacobian determinant matrix of the DIR motion field. Greater values of $CTVI_{DIR-Jac}(x)$ indicate greater lung expansion, which is taken as proportional to ventilation.

Non-DIR HU metric ($CTVI_{HU}$)

The third metric represents a streamlined form of CTVI that estimates physiological ventilation (i.e. blood-gas exchange) in terms of the voxel-wise product of tissue and air densities [11]. We calculated this on each exhale phase image using,

$$CTVI_{HU}(x) = \left[\frac{HU_{exhale}(x)}{-1000}\right] \times \left[\frac{HU_{exhale}(x) + 1000}{1000}\right]$$

where the first term on the RHS gives the fractional air content and the second term gives the fractional tissue content.

x

Ventilation image alignment and post processing

In order to perform voxel-to-voxel comparisons between CTVI and Galligas PET, we used 3DSlicer version 4.4 (http://www.slicer.og) to perform a manual rigid alignment of each PET scan to the corresponding exhale BHCT and separately to the exhale 4DCT. Since the attenuation correction CT was not saved for retrospective analysis, the alignment was visually assessed based on image features in normally ventilated lung. Since each set of 4DCT, BHCT and Galligas PET scans were completed within 20 min in a single session and on the same scanner, only longitudinal shifts along the direction of couch motion were needed. No significant attenuation correction motion artefacts were noted.

In order to limit the ventilation image comparisons to lung voxels only, high quality lung masks were generated on the exhale phase of each BHCT and 4DCT scan using an in-house IDL-based semi-automated algorithm implemented on a HERMES workstation (Hermes Medical Solutions, Sweden).

The main airways were manually brushed out using ITK Snap (http://www.itksnap.org) and the resulting masks were verified by a radiologist. We point out that the high quality lung masks generated here are distinct to the coarse masks used in our DIR/CTVI pipeline. Only lung voxels present in both masks were included in the Spearman correlation analysis.

A mask-preserving median filter of dimensions 7 x 7 x 7 voxels^3 was applied to all the ventilation images. The filter size is representative of other CTVI studies, with parameters selected to minimise the impact of image noise without degrading the spatial fidelity of the ventilation images. By comparison, the original paper by Guerrero et al. [2] applied a box average filter of 3 x 3 x 3 mm^3 whereas Kida et al. [10] used a 9 x 9 x 3 voxel^3 Gaussian kernel.

Semi quantitative DIR evaluation

DIR results were verified based on qualitative and quantitative metrics suggested by the AAPM Task Group 132 [19]. Qualitative assessment involved the use of image overlays to compare the alignment of high contrast lung features before and after DIR. We also inspected the DIR motion field for instances of non-physiologic motion (e.g. folding of tissue), which is indicated by negative values of the Jacobian determinant. We found that 0.84% of 4DCT lung voxels exhibited negative Jacobian values; for three scans this was between 1% and 5% of all lung voxels; how- ever, the issue was not considered significant enough to exclude these scans. The majority of negative Jacobian values occurred where lung anatomy was truncated from the 4DCT scan, e.g. near the diaphragm. By comparison, the BHCT scans were completely free of negative Jacobian values in the lung.

Comparisons with Galligas PET

The CTVI accuracy was evaluated using the Spearman correlation coefficient (r), which we use to describe the monotonicity of ventilation values in spatially matched voxels between CTVI and Galligas PET. We used MATLAB R2015a (Mathworks Inc.) to calculate the Spearman r values for each of the BHCT- and 4DCT- ventilation images ($CTVI_{DIR-HU}$, $CTVI_{DIR-Jac}$ and $CTVI_{HU}$) with the corresponding Galligas PET scan. Similar to the classifications proposed by Dawson et al. [20], we refer to r >0.75 as ‘‘strong”, r = 0.5–0.75 as ‘‘good”, r = 0.25–0.5 as ‘‘moderate” with $r < 0.25$ indicating ‘‘weak or no relationship”. For the 13 patients where BHCT and 4DCT scans were both successfully acquired, we applied a series of two-tailed t-tests to compare the distribution of r-values for any given CTVI method. The null hypothesis was that BHCT and 4DCT did not lead to significantly different r-values; the significance level was set at p = 0.05.

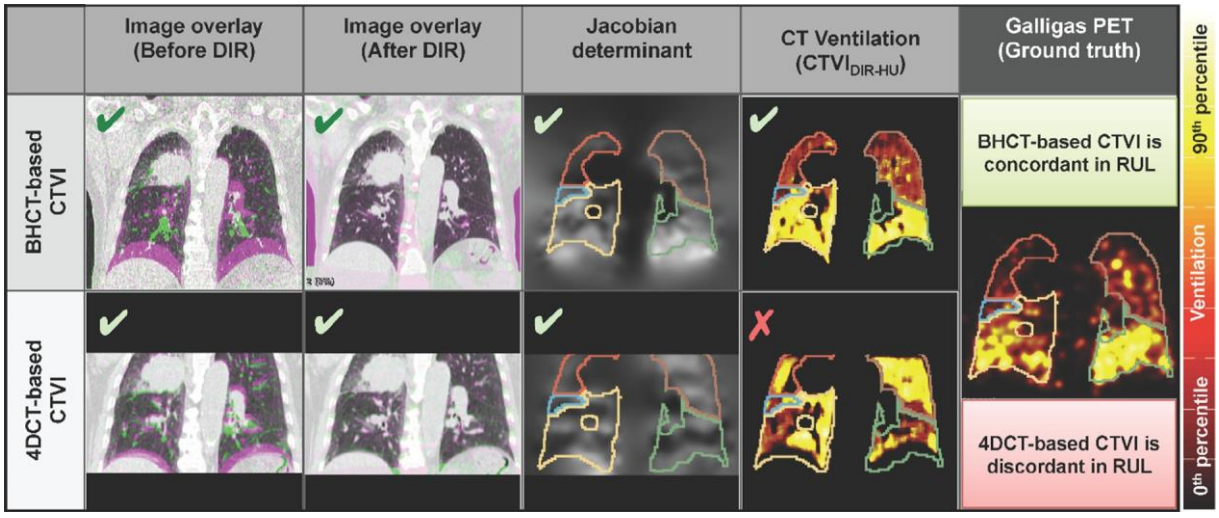

Fig. 2. Comparing CTVIs derived from BHCT (upper row) and 4DCT (lower row). From left to right: image overlay (before DIR), image overlay (after DIR), Jacobian determinant, $CTVI_{DIR-HU}$, and Galligas PET. All images show the same coronal plane; For ease of viewing, all ventilation images were normalised based on the 90th percentile ventilation in the lung. Spearman *r*-values evaluated versus Galligas PET were 0.55 for BHCT and −0.04 for 4DCT.

Results

Qualitatively, BHCT derived CTVIs achieved better visual concordance with Galligas PET compared to 4DCT derived CTVIs. Fig. 2 shows a comparison of BHCT- and 4DCT-derived CTVIs for a representative patient with a right upper lobe (RUL) tumour obstruction defect. The figure shows image overlays of the exhale/inhale CT phase images before and after DIR (first and second columns from the left, respectively), the Jacobian determinant and $CTVI_{DIR-HU}$ in each case (third and fourth columns) as well as the ground truth Galligas PET scan (fifth column). All images show the same coronal plane with ventilation images normalised based on the 90th percentile value in the lung. For both BHCT and 4DCT conditions, the image overlays suggest acceptable image quality before DIR, acceptable alignment of anatomic structures after DIR and an acceptable Jacobian determinant image (no singularities), all indicated by green ticks in the panels of the figure. In terms of the CTVI however, only the BHCT-based $CTVI_{DIR-HU}$ provides good concordance with Galligas PET in terms of the RUL defect. By comparison the 4DCT-based $CTVI_{DIR-HU}$ has an inverted distribution between RUL and the right middle lobe (RML) and right lower lobe (RLL).

Fig. 3 shows additional visual comparisons between the BHCT-based $CTVI_{DIR-HU}$ and Galligas PET for four patients with different levels of function impairment (based on clinical COPD and D_{LCO} abnormality). Also shown is the per-lobe contribution to total lung function, as calculated using the same approach as in our earlier CTVI study [13]. We observe good visual concordance between CTVI and Galligas PET and similar lobar distributions. A few regions of disagreement appear to coincide with non-severe clumping artefacts in the Galligas PET scans (indicated by red arrows in the figure).

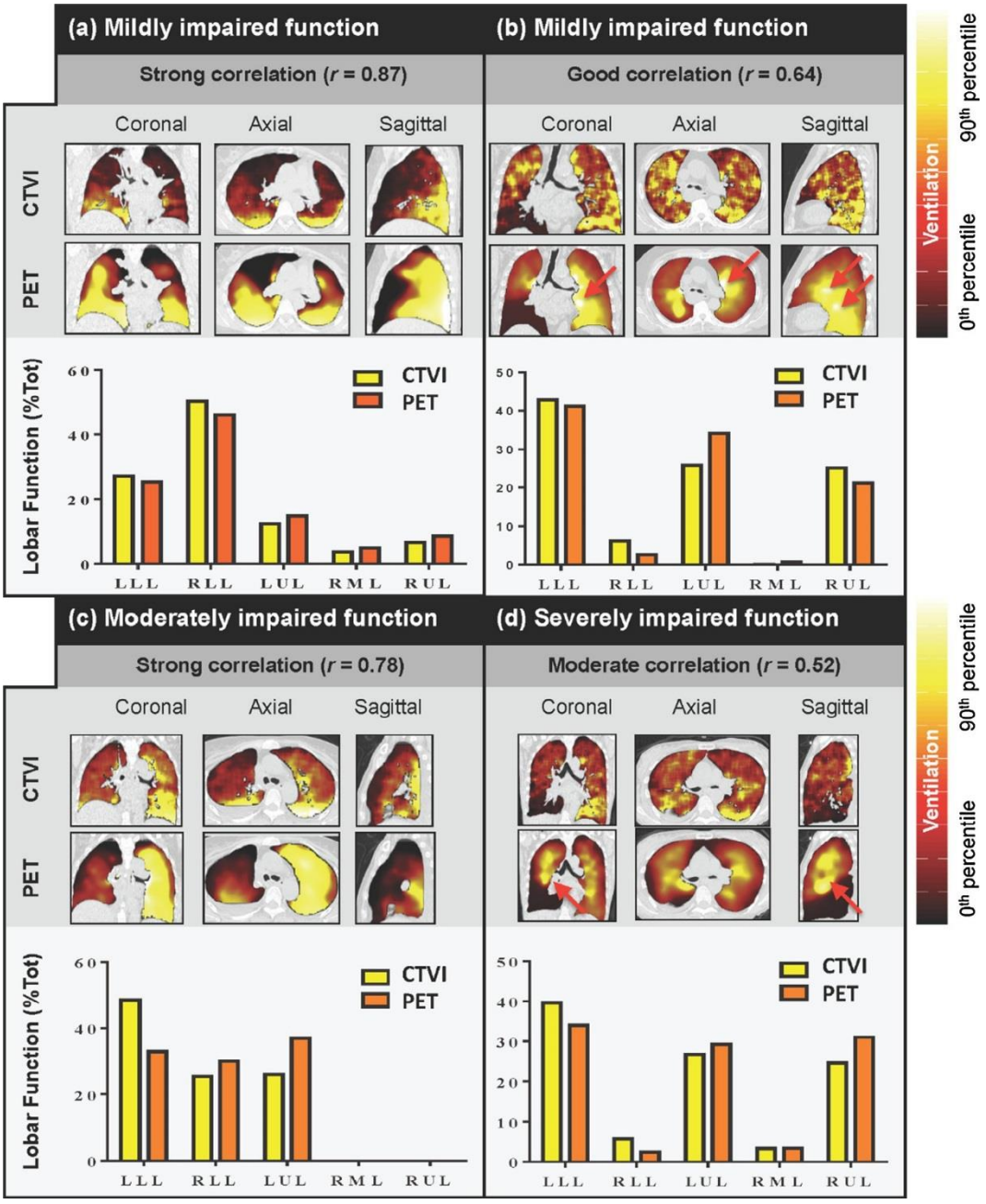

Fig. 3. Comparing BHCT-based CTVI and Galligas PET for different cases (a)–(d) of lung function impairment. In each case, the upper row shows $CTVI_{DIR-HU}^{BHCT}$ and the lower row shows Galligas PET. Red arrows show suspected clumping in Galligas PET. For ease of viewing, all ventilation images were normalised based on the 90th percentile ventilation in the lung. The bar plots show the contribution to total lung function from each lobe. LLL = left lower lobe, RLL = right lower lobe, LUL = left upper lobe, RML = right middle lobe and RUL = right upper lobe

Quantitatively, the Spearman correlation results for both BHCT-derived and 4DCT-derived CTVIs are shown in the boxplot of Fig. 4 (data for the $7 \times 7 \times 7$ voxel^3 median filter is shown). For each box the upper, middle and lower edges show the 75th, median and 25th percentile of Spearman *r* values averaged over all 16 patients. BHCT-derived CTVIs (white boxes) showed overall higher accuracy than 4DCT-derived CTVIs (shaded boxes). The best overall *r*-values were achieved by the $CTVI_{DIR-HU}^{BHCT}$ method, with a mean (range) of 0.67 (0.52–0.87). This was followed by $CTVI_{DIR-Jac}^{BHCT}$ and $CTVI_{HU}^{BHCT}$, with 0.57 (0.18–0.77) and 0.49 (0.14–0.75), respectively. By comparison, 4DCT-based CTVIs achieved $\bar{r}$=0.32 (−0.04 to 0.51) for the $CTVI_{DIR-HU}^{4DCT}$ method, 0.16 (−0.31 to 0.44) for $CTVI_{DIR-Jac}^{4DCT}$ and 0.49 (0.20–0.77) for $CTVI_{HU}^{4DCT}$. Notably the $CTVI_{HU}$ method, which does not rely on DIR, proved the least accurate of the BHCT-derived CTVIs but was the most accurate of the 4DCT-derived CTVIs.

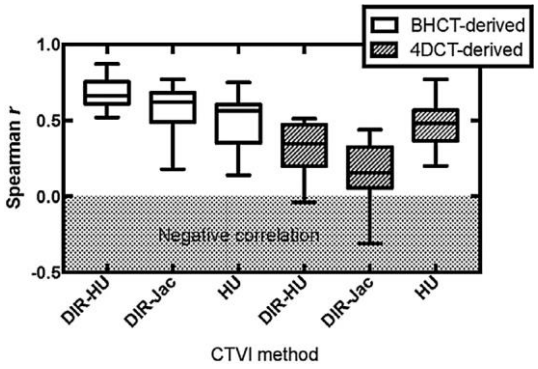

Fig. 4. Box plot of the Spearman correlations between each type of CTVI and the corresponding Galligas PET scan. Different CT modalities (BHCT and 4DCT) and different CTVI methods (DIR-HU, DIR-Jac and HU) are shown.

Comparing only those patients with matched BHCT and 4DCT scans ($N = 13$), we observe similar trends as for the whole cohort. That is, the $CTVI_{DIR-HU}^{BHCT}$, $CTVI_{DIR-Jac}^{BHCT}$ and $CTVI_{HU}^{BHCT}$ methods achieve mean (range) *r* values of 0.67 (0.55–0.87), 0.58 (0.36–0.77) and 0.51 (0.14–0.75) respectively, whereas the $CTVI_{DIR-HU}^{4DCT}$, $CTVI_{DIR-Jac}^{4DCT}$ and $CTVI_{HU}^{4DCT}$. methods achieved lower values of 0.31 (−0.04–0.51), 0.14 (−0.31 to 0.44) and 0.50 (0.20–0.77) respectively. Applying a series of *t*-tests to this data, we find that when using either of the DIR-based methods $CTVI_{DIR\text{-}HU}$ or $CTVI_{DIR\text{-}Jac}$, the choice of BHCT or 4DCT leads to significant differences in the CTVI accuracy ($p < 0.001$). However when using the non-DIR method, $CTVI_{DIR\text{-}HU}$, the choice of BHCT or 4DCT did not have a significant impact on CTVI accuracy ($p = 0.66$).

From Fig. 2 we can see that the BHCT and 4DCT images can suffer some truncation of the lung field of view (FOV) and this arises through the clinical 4DCT scan protocol. As a result it is useful to separate out the potential impact of the FOV truncation from that of image quality. To investigate this, we re-calculated all of the BHCT-derived CTVIs by first manually aligning each BHCT scan to the corresponding 4DCT scan and then truncating the BHCT to provide the same axial FOV as the 4DCT. We found that the truncation of exhale lung volumes in the 4DCT scans was variable, with a mean (range) of 12% (0–35%) compared to the full-FOV BHCT scans which suffered no truncation. Truncating the BHCT scans in this manner did result in lower Spearman correlations with Galligas PET: mean correlations for the DIR-HU method were reduced from -0.67 (before truncation) to 0.56 (after truncation), and correlations for the DIR-Jac method were reduced from 0.57 to 0.28. The accu- racy of CTVI computed from truncated BHCT scans was still better than CTVI derived from 4DCT scans, suggesting that image

quality differences had a larger impact than FOV differences in this patient cohort.

Discussion

4DCT-based CTVI has been proposed as an accessible tool for functionally adaptive treatment planning in the radiotherapy treatment of lung cancer. The deleterious impact of irregular breathing in clinical 4DCT has meant that voxel-level accuracy for CTVI could not be reliably demonstrated in humans. The goal of this study was to evaluate an improved CTVI method derived from exhale/inhale breath hold CT (BHCT) scans and assessed against a proven ventilation imaging method, Galligas PET. By acquiring each patient's exhale/inhale BHCT, 4DCT and Galligas PET scans in a single imaging session on the same scanner, we have performed the first direct comparison of BHCT- and 4DCT-based CTVIs vs. nuclear medicine, whilst also minimising time-delays and patient setup differences across the three imaging modalities. Our analyses suggest that BHCT-based CTVIs can demonstrate better voxel level accuracy than those based on 4DCT, especially when that CTVI is generated using DIR ($p < 0.001$). It is intuitive that the impact of 4DCT image artefacts will be more severe for DIR-based CTVI methods, if the underlying evaluation of regional intensity or volume change is based on two (or more) artefact- ridden phase images. It is challenging to establish 4DCT image quality metrics that can predict errors in CTVI [12,15]. Furthermore CTVI errors may not always be immediately obvious. For example Fig. 2 shows discordant ventilation distributions between the 4DCT-based CTVI and the Galligas PET scan, despite no obvious issues with the underlying DIR result. By comparison the simple HU-based method $CTVI_{HU}$, which does not use DIR and was calculated only from the stable exhale phase, showed no significant difference in accuracy between BHCT or 4DCT ($p = 0.66$). This is in accordance with earlier Galligas PET and Technegas SPECT studies [11,12].

From the perspective of the radiotherapy planning workflow, the main limitation of BHCT is that it represents an additional (albeit small) imaging dose on top of 4DCT. Many commercial 4DCT scanners are capable of acquiring both 4DCT and breath- hold scan modes so the additional time-burden should be minimal. A second limitation of BHCT is that not all patients will be able to achieve a full breath-hold for the 10 s required for each exhale/ inhale scan. In this study patients received Audio-visual guidance to achieve breath holds at 80% of maximum inhalation and exhalation. These targets were based on previous experience of patients' capabilities and also taking into account the limitations of our DIR tools in dealing with large breathing amplitudes. It is possible that duration and amplitude for the exhale/inhale breath holds could be further optimised in future studies.

We point out that for non-radiotherapy applications such as surgical risk assessment, where it is acceptable to evaluate ventilation at more coarse (lobar) distance scales, the efficacy of 4DCT- based CTVI has already been demonstrated. For these applications, the main advantages of BHCT-based CTVI will be (typically) lower imaging dose compared to 4DCT, and greater accessibility outside of radiotherapy departments.

Conclusion

This study assessed the spatial accuracy of CT ventilation imaging (CTVI) versus Galligas PET scans for 16 lung cancer patients using a combined 4DPET/CT scanner. We found that CTVIs created from exhale/inhale breath hold CT scans showed significantly higher spatial accuracy compared to clinical 4DCT. These results suggest that high quality CT imaging will be a key component for accurate CTVI.

.

References

1) Gefter WB, Hatabu H. Functional lung imaging: emerging methods to visualize regional pulmonary physiology. Acad Radiol 2003;10:1085–9.

2) Guerrero T, Sanders K, Castillo E, Zhang Y, Bidaut L, Pan TS, et al. Dynamic ventilation imaging from four-dimensional computed tomography. Phys Med Biol 2006;51:777–91.

3) Reinhardt JM, Ding K, Cao K, Christensen GE, Hoffman EA, Bodas SV. Registration-based estimates of local lung tissue expansion compared to xenon CT measures of specific ventilation. Med Image Anal 2008;12:752–63.

4) Yamamoto T, Kabus S, von Berg J, Lorenz C, Goris M, Loo BW, et al. Evaluation of four-dimensional(4D) computed tomography (CT) pulmonary ventilation imaging by comparison with single photon emission computed tomography (spect) scans for a lung cancer patient. Third International Workshop on Pulmonary Image Analysis; 2010.

5) Castillo R, Castillo E, Martinez J, Guerrero T. Ventilation from four-dimensional computed tomography: density versus Jacobian methods. Phys Med Biol 2010;55:4661–85.

6) Vinogradskiy Y, Koo PJ, Castillo R, Castillo E, Guerrero T, Gaspar LE, et al. Comparison of 4-dimensional computed tomography ventilation with nuclear medicine ventilation-perfusion imaging: a clinical validation study. Int J Radiat Oncol Biol Phys 2014;89:199–205.

7) Yamamoto T, Kabus S, Lorenz C, Mittra E, Hong JC, Chung M, et al. Pulmonary ventilation imaging based on 4-dimensional computed tomography: comparison with pulmonary function tests and SPECT ventilation images. Int J Radiat Oncol Biol Phys 2014;90:414–22.

8) Kipritidis J, Siva S, Hofman MS, Callahan J, Hicks RJ, Keall PJ. Validating and improving CT ventilation imaging by correlating with ventilation 4D-PET/CT using Ga-68-labeled nanoparticles. Med Phys 2014;41.

9) Brennan D, Schubert L, Diot Q, Castillo R, Castillo E, Guerrero T, et al. Clinical validation of 4-dimensional computed tomography ventilation with pulmonary function test data. Int J Radiat Oncol Biol Phys 2015;92:423–9.

10) Kida S, Bal M, Kabus S, Negandar M, Shan X, Loo BW, et al. CT ventilation functional image-based IMRT treatment plans are comparable to SPECT ventilation functional image-based plans. Radiother Oncol 2016;118:521–7.

11) Kipritidis J, Hofman MS, Siva S, Callahan J, Le Roux PY, Woodruff HC, et al. Estimating lung ventilation directly from 4D CT Hounsfield unit values. Med Phys 2016;43:33–43.

12) Hegi-Johnson F, Keall P, Barber J, Bui C, Kipritidis J. Evaluating the accuracy of 4D-CT ventilation imaging: first comparison with technegas SPECT ventilation. Med Phys 2017.

13) Eslick EM, Bailey DL, Harris B, Kipritidis J, Stevens M, Li BT, et al. Measurement of preoperative lobar lung function with computed tomography ventilation imaging: progress towards rapid stratification of lung cancer lobectomy patients with abnormal lung function. European journal of cardio-thoracic surgery; 2015.

14) Yamamoto T, Langner U, Loo BW, Shen J, Keall PJ. Restrospective analysis of artifacts in four-dimensional CT images of 50 abdominal and thoracic radiotherapy patients. Int J Radiat Oncol Biol Phys 2008;72:1250–8.

15) Yamamoto T, Kabus S, Lorenz C, Johnston E, Maxim PG, Diehn M, et al. 4D CT lung ventilation images are affected by the 4D CT sorting method. Med Phys 2013;40.

16) Tahir BA, Van Holsbeke C, Ireland RH, Swift AJ, Horn FC, Marshall H, et al. Comparison of CT-based lobar ventilation with He-3 MR imaging ventilation measurements. Radiology 2016;278:585–92.

17) Bailey DL, Eslick EM, Schembri GP, Roach PJ. Ga-68 PET ventilation and perfusion lung imaging-current status and future challenges. Semin Nucl Med 2016;46:428–35.

18) Kipritidis J, Woodruff H, Eslick E, Hegi-Johnson F, Keall PJ. New pathways for end-to-end validation of CT ventilation imaging (CTVI) using deformable image registration. IEEE 13th International Symposium on Biomedical Imaging (ISBI); 2016;April.

19) Brock KK, Mutic S, McNutt TR, Li H, Kessler ML. Use of image registration and fusion algorithms and techniques in radiotherapy: Report of the AAPM Radiation Therapy Committee Task Group No. 132.. Med Phys 2017.

20) Dawson Beth, G. TR. Basic & Clinical Biostatistics, 4th ed., Lange Medical Books/ McGraw-Hill; 2004.